International Journal of Academic Engineering Research (IJAER)
ISSN: 2643-9085
Vol. 9 Issue 8 August - 2025, Pages: 192-201

An Enhanced PID Based Electrical Fault Detection System for Three Phase Induction Motor

Kennedy Ihemba[1], Ekene Samuel Echefu[1], I. U. Uju[2]

[1]Department of Electrical and Electronic Engineering, Federal Polytechnic Nekede, Owerri, Nigeria
[2]Department of Electrical and Electronic Engineering, Chukwuemeka Odumegwu Ojukwu University, Uli, Nigeria

Abstract: *As the main components of several industrial and commercial systems, correct and reliable operation and performance of induction is inevitable for efficiency and increased production. Also, having fault detection scheme is of significant and brings valuable advantage by enhancing performance and ensuring that motor is prevented from damage when fault occurs. In this work, an electrical fault detection system for three phase induction motor is proposed. The system was basically designed to detect electrical fault (short-circuit) between any phase and the ground. In order to achieve this, control circuit based on discrete Proportional, Integral and Derivative (PID) controller with low pass filter as part of the derivative element called PIDf was designed. The designed PIDf controller was tied to trip-off circuit (or circuit breaker) such that it provides a command signal that enables the circuit to trip-off and then cut the motor off the supply when fault condition sets in such as fault voltages, faults current or fault voltages and currents. A Root Mean Square (RMS) technique that functioned to evaluate the harmonics present in the voltage or current waveform by so doing determine the quality of the output voltage or current, which then helps to detect the type of fault, was incorporated as part of the feedback network to the controller. Thus, the resulting type of fault is displayed on a scope attached to the RMS. The entire system with three-phase induction was modelled in MATLAB/Simulink. Simulations were initially conducted when the motor was running normally without any short circuit fault in the supply line. The results revealed that the starting current was high as shown by the rotor and stator currents, low starting torque and with the motor running at the rate speed of 1500 rpm. Further simulations were conducted for fault analysis without the controller as part of the system and the results revealed that the motor decreased from 1500 rpm to 1470 rpm for single-phase short circuit fault, 1500 rpm to 1365 rpm two-phase short circuit fault, and 1500 rpm to 1325 rpm for three-phase short circuit fault occurred. the integration of the designed discrete time proportional-integral-derivative (PID) controller with low pass derivative filter (that is PIDf) ensures that detected error (or fault) signal is applied to the circuit breaker to cut off the motor from the network when any of these faults occurred. Thus, the resulting output of the motor is zero. As shown by the RMS technique, the occurrence of short circuit caused voltage sag along the supply line. Generally, the application of the discrete PIDf controller provided not only fault detection, but protection for the motor by ensuring that the circuit breaker trip off the line connection to the motor.*

Keywords—PID controller, Induction motor, Fault detection, Root mean square, Speed

1. INTRODUCTION

Electrical induced faults in three phase induction motor are faults that will cause increased heat on both stator and rotor windings [1]. These faults may be over current or over load), unbalance voltage, over/under voltage, phase reversing, single phasing, and earth fault. Mechanical induced faults are faults that are caused by failure of winding, stator winding, and bearing faults. These failures are the most common mechanical faults in three phase induction motor [2]. Environmental induced faults consist of contamination, external moisture, and ambient temperature. The performance of induction motor under various operations is also affected by the vibration of the machine.

The most common faults in three-phase induction motor are the electrical related types, and will produce more heat on both stator and rotor winding. This results in decreasing of induction motor life time. In this work, the dynamic characteristics of three-phase induction motor under the effect of unbalanced supply voltage, single phasing and over load condition are examined. This work is designed to provide much easier approach to simulate the dynamic characteristics of electrical faults using Simulink and Power System Blocks of MATLAB simulation software than the conventional techniques that involves the use of analog devices such as operational amplifiers and potentiometer as in [1].

In order to protect motor from more heating as a result of these electrical faults, protection technique designed to protect each and every individual fault with separate protective relay such as earth fault relay and over current relay and so on is implemented. This approach will be very expensive and not cost effective. In order to Overcome this cost burden in the management of electrical faults in three-phase induction motor, a technique requiring a low cost, reliable and integrated protection mechanism is developed for three-phase induction motor using enhanced Proportional-Integral-Derivative (PID) controller is developed in this work.

The remaining part of this paper is divided into four sections: literature review, system design, results and discussion, and conclusion.

International Journal of Academic Engineering Research (IJAER)
ISSN: 2643-9085
Vol. 9 Issue 8 August - 2025, Pages: 192-201

2. LITERATURE REVIEW

Control systems are largely employed in electrical machines to for various purposes. For instance, model predictive control has been used with vector control to enhance the performance of permanent magnet synchronous motor [3]. The stability of rotor angle in synchronous generators was achieved using neuro-fuzzy excitation control system [4]. Optimal control technique was used to minimize energy consumption of squirrel cage induction motor [5]. Voltage and frequency speed control system was used to improve the performance of three-phase induction motor [6]. Other significant studies related induction motor are in existing literature. These studies have been carried out with respect to induction motor. These include: dynamic modelling to examine transient response performances via simulation such as in [7], the use of double-cage rotor induction motor to enhance dynamic response [8], and rotor temperature analysis for single-cage and double-cage induction three-phase induction motor [9]. However, these approaches did not address the possible electrical faults in three-phase induction motor. Hence, some approaches have been implemented. For instance, PIC microcontroller-based control system was used for a three-phase induction motor protection [10]. Control scheme based on LM 324 operational amplifier configured in comparator mode was used in providing protection for three phase induction motor from external faults [1]. Techniques based on based on fuzzy logic, Artificial Neural Network (ANN), and combined fuzzy logic and ANN called neuro-fuzzy were used to provide three phase induction motor fault diagnosis [11]. A scheme that facilitates fault detection in induction motor by inter-switching of multiple controllers was presented by Abubakar *et al.* [12]. Microcontroller was designed for the protection of induction motor from faults such as single phasing, over heat, and over current [13] and also for single phasing faults, under voltage, and unbalance voltage [14]. In the study by Chouhan *et al.* [15], five mechanical faults, four electrical faults and one healthy motor condition were examined using ANN. Wavelet and fuzzy controller for induction motor faults detection and classification was implemented by Umap and Bobade [16].

The empirical review has shown that while recent studies have been directed towards protection of induction motor from operational failures induced by electrical faults such as over voltage, under voltage, over current, unbalance voltage, phase reversing, and earth faults. However, while all the reviewed studies have reported promising remarks about the proposed systems, less or no attention has been given to the effect of these systems regarding speed control performance of induction motor. This is because the speed of motor will certainly be affected by faults in stator winding when it occurs. In this work, a system will be designed to address the effect of induction motor speed control considering changing load torque while providing fault protection of the system.

3. SYSTEM DESIGN

The architecture of the proposed fault protection system for three phase induction motor is shown in Fig. 1. The structure is a block diagram of a three-phase induction motor connected to three phase alternating current supply line via an intermediate circuit that provide a trip-off function when fault occurs. Then the control circuit (PIDf) is tied to trip-off circuit such that the controller provides a command signal that enables the circuit to trip-off and then cut the motor off the supply when fault condition sets in such as fault voltages, faults current or fault voltages and currents. The RMS technique functions to evaluate the harmonics present in the voltage or current waveform by so doing determine the quality of the output voltage or current, which then helps to detect the type of fault. The resulting type of fault is displayed on a scope attached to the RMS.

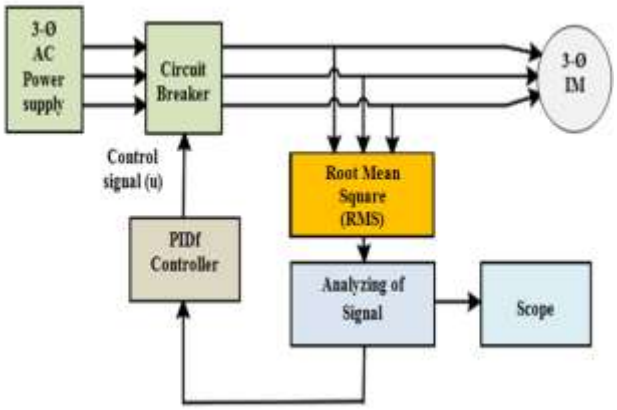

Fig. 1. *Proposed fault protection system for induction motor*

3.1 Mathematical Modelling of Induction Motor

The mathematical derivation of equations representing the dynamic equivalent circuit of induction machine can be realized using d-q reference axis assumption as shown in Fig. 2 to 4.

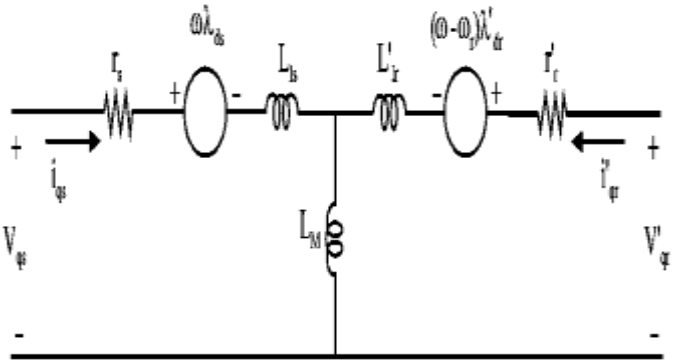

Fig. 2. *q-axis of induction motor*

International Journal of Academic Engineering Research (IJAER)
ISSN: 2643-9085
Vol. 9 Issue 8 August - 2025, Pages: 192-201

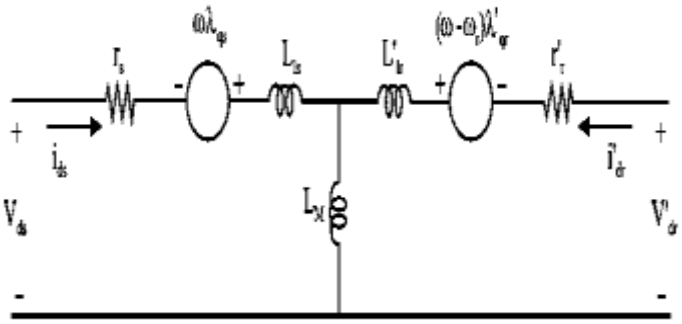

Fig. 3. *d-axis of induction motor*

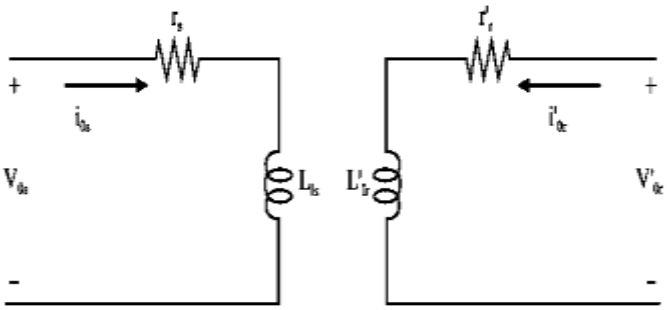

Fig. 4. *Equivalent circuit of a three-phase induction motor*

The voltage equations of the stator and rotor in d-axis and q-axis are given by Sudha and Anbalagan [2]:

$$V_{qs} = r_s i_{qs} + \omega\lambda_{ds} + p\lambda_{qs} \quad (1)$$

$$V_{ds} = r_s i_{ds} - \omega\lambda_{qs} + p\lambda_{ds} \quad (2)$$

$$V_{0s} = r_s i_{0s} + +p\lambda_{0s} \quad (3)$$

$$V_{qr}^{'} = r_r^{'} i_{qr}^{'} + (\omega\text{-}\omega_r)\lambda_{dr}^{'} + p\lambda_{qr}^{'} \quad (4)$$

$$V_{qr}^{'} = r_r^{'} i_{qr}^{''} - (\omega - \omega_r)\lambda_{qr}^{'} + p\lambda_{dr}^{'} \quad (5)$$

$$V_{0r}^{'} = r_r^{'} i_{0r}^{'} + p\lambda_{0r}^{'} \quad (6)$$

The flux linkage equations for the stator and rotor are given by:

$$\lambda_{qs} = L_{ls} i_{qs} + M\left(i_{qs} + i_{qr}^{'}\right) \quad (7)$$

$$\lambda_{ds} = L_{ls} i_{ds} + M\left(i_{ds} + i_{dr}^{'}\right) \quad (8)$$

$$\lambda_{0s} = L_{ls} i_{0s} \quad (9)$$

$$\lambda_{qr}^{'} = L_{lr}^{'} i_{qr}^{'} + M\left(i_{qs} + i_{dr}^{'}\right) \quad (10)$$

$$\lambda_{dr}^{'} = L_{lr}^{'} i_{dr}^{'} + M\left(i_{ds} + i_{dr}^{'}\right) \quad (11)$$

$$\lambda_{0r}^{'} = L_{lr}^{'} i_{0r}^{'} \quad (12)$$

where V_{qs}, V_{ds}, V_{0s}, $V_{qr}^{'}$, $V_{dr}^{'}$, $V_{0r}^{'}$ are the voltages of stator and rotor in d-q axis reference including the zero reference (which may not be present), λ_{ds}, λ_{qs},$\lambda_{dr}^{'}$and $\lambda_{qr}^{'}$are the flux linkages for the stator d-axis/q-axis and the rotor d-axis/q-axis,i_{ds},i_{qs}, $i_{dr}^{'}$ and $i_{qr}^{'}$ are the stator current for d-axis/q-axis and the rotor current for d-axis/q-axis respectively.

3.2 Controller Design

An appropriate controller used in industrial process control and automation to provide three-term control loop feedback mechanism is the Proportional-Integral-Derivative (PID) controller. This control technique reduces error of system by adjusting the process with the aid of a control or command signal u(t). PID controller guarantees optimum control action as well as zero steady state error, reduced rise time (or fast response), minimized overshoot, near zero oscillation and better stability. The use of PID controller is common in higher order plants and this is the main advantage it has over some other linear controller including its ease of design and implementation. Fig. 5 is a simplified block diagram of PID control system.

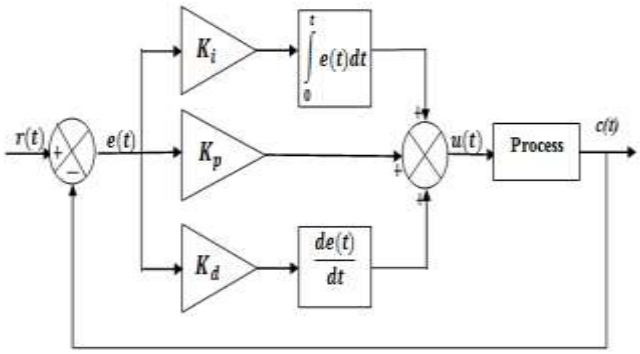

Fig. 5. *Block diagram of PID control system*

The mathematical description of PID control scheme can be determined considering Fig. 5. The variables $r(t)$,$e(t)$,$u(t)$ are the reference input, error and control signal. AlsoK_p,K_i,K_d are proportional, integral and derivative gains and represents the parameters of the PID controller, and $c(t)$ is the output. Thus, the difference between the reference input r(t) and the actual output c(t) is the error signal and it is given by:

$$e(t) = r(t) - c(t) \quad (13)$$

The error is subjected to three computational operations involving direct scaling, integration and derivation, with each action performed to compensate the weakness of the others and as such a signal u(t) that is more refined and suitable to force corrective action on the plant or process is produced. The control signal is given as [17]- [19]:

$$u(t) = K_p e(t) + K_i \int_0^t e(t)\mathrm{d}t + K_d \frac{\mathrm{de}(t)}{\mathrm{dt}} \quad (14)$$

Equation (14) is the expression for control signal in continuous time form. It can be expressed in complex frequency s-domain using Laplace transformation and assuming zero initial condition by:

$$U(s) = K_p E(s) + K_i \frac{1}{s} E(s) + K_d \mathrm{sE}(s) \quad (15)$$

The PID controller is given as [20]- [22]:

$$C_{\mathrm{pid}}(s) = K_p + K_i \frac{1}{s} + K_d s \quad (16)$$

However, the real PID control technique is often implemented with a pre-filter added to the derivative element to address the problem of noise that could go into the controller through the derivative part in practice [17]. Therefore, the real PID is given by:

$$C_{\mathrm{pid}}(s) = K_p + K_i \frac{1}{s} + K_d \left(\frac{s}{s+1/N}\right) \quad (17)$$

Equation (17) is the continuous time real PID controller with N filter coefficient. However, in this work a discrete time (digital) component of the real PID controller is implemented and it is obtained by performing z-transform of Equation (17) for a sampling time T_s given by Eze *et al.* [20]:

$$C_{\text{pid}}(z) = K_p + K_i\left(\frac{T_s}{z-1}\right) + K_d\left(\frac{(z\text{-}1)N}{z-1+\text{NT}_s}\right) \quad (18)$$

The values for the tuned parameters of the discrete time PID controller are $K_p = 60$, $K_i = 1400$, and $K_d = 1.0$. The sampling time for zero-order hold (ZOH) circuit used for the conversion of the PID from continuous time system to discrete time system $T_s = 0.00005\ sec$. The filter coefficient is N = 10. Substituting these values into Equation (18) gives the designed PID controller:

$$C_{\text{pid}}(z) = 60 + 1400\left(\frac{0.00005}{z-1}\right) + \left(\frac{10(z\text{-}1)}{z-0.995}\right) \quad (19)$$

This section has presented the control technique that will be used to provide protection for the three-phase induction motor.

3.3 Root Mean Square Voltage

The root mean square (RMS) computed at each half cycle $V_{rms_{(1/2)}}$ is determined from the voltage samples in the time domain as expressed by Candelo and Montaña [23]:

$$V_{rms_{(1/2)}} = \sqrt{\frac{1}{N}\sum_{1=1}^{N} v_i} \quad (20)$$

where i corresponds to each sample, N is the total number of samples, and v_i is the voltage value in the time domain. The value is updated every half cycle. Most measurement devices use the lower value of $V_{rms_{(1/2)}}$ is computed each half cycle in the time domain as the voltage sag magnitude [23].

The three-phase squirrel cage induction motor is considered in this work using the following specifications presented in Table 1.

Table 1: Simulation parameters

Parameter definition	*Value*	*Unit*
Power rating	37.3	kW
Line voltage	380	V
Frequency	50	Hz
Rated speed	1500	rpm
Connection	-	Delta
Class	-	E
Number of poles (p)	2	poles
Stator resistance (r_s)	3.5	Ω
Rotor resistance (r_r)	3.16	Ω
Mutual inductance (M)	0.26	H
Stator and rotor linkage reactance (X_{1s}), (X_{1r})	0.0068	H

4. RESULTS

The simulation results obtained from the analysis carried out regarding electrical fault detection in an induction motor running at a given speed when fed by a three-phase power supply unit is presented in this chapter. The simulation analysis has been considered for three given scenarios. The first scenario considered the motor to operating under normal condition. In the second and third cases, the system was evaluated at the instance that designed PIDf controller was integrated and when it was not for the three electrical faults considered. Short circuit (electrical) faults were modelled using fault block parameters of the MATLAB/Simulink. Thus, with the aid of this block, each short circuit fault, single-phase short circuit, two-phase short circuit, and three-phase short circuit can be modelled. All analysis was conducted assuming no load condition.

4.1 Normal Operation of Induction Motor

In this section, the performance of the three-phase motor is evaluated assuming it was running with any line fault in form of short circuit. Fig. 6 shows the simulation analysis during normal operation of the motor in terms of rotor current, stator current, electromechanical torque and speed of the motor.

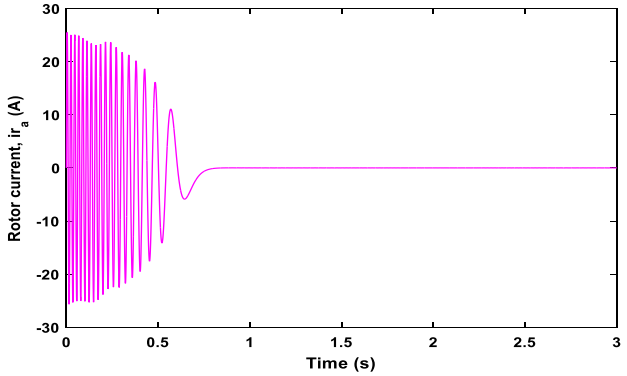

Fig. 6a. Rotor current at normal operation

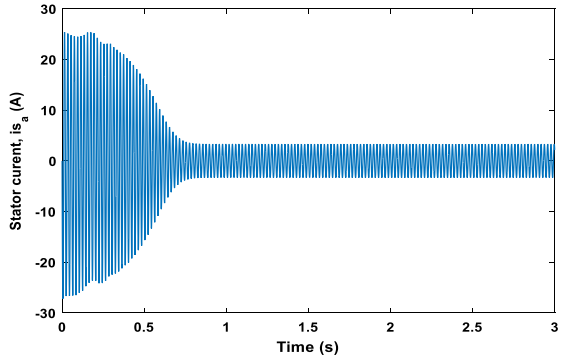

Fig. 6b. Stator current at normal operation

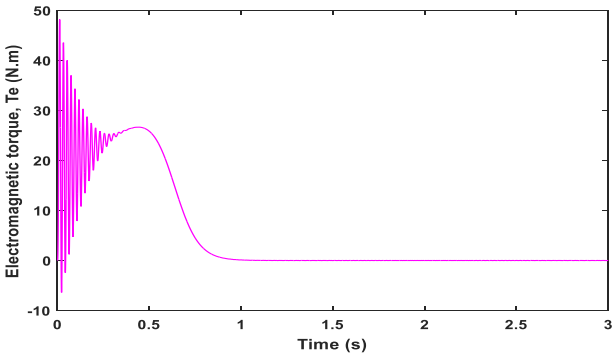

Fig. 6c. Electromechanical torque at normal operation

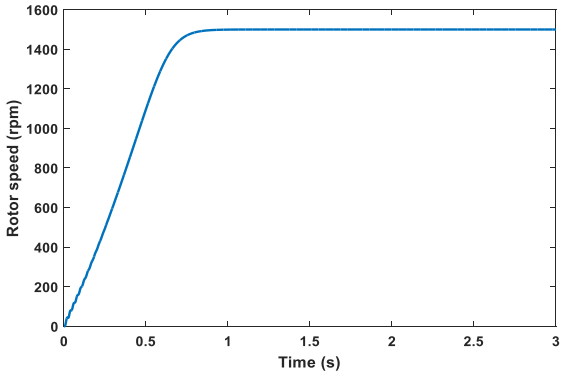

Fig. 6d. Electromechanical torque at normal operation

Fig. 6. Performance characteristics of the motor in normal operation

The simulation curves for the performance of the motor during normal operation indicate that the starting current was high, which makes the rotor and the stator currents to be initially high 25.3 A but gradually drops to near zero as the machine approaches it rated speed. The same holds for the electromechanical torque, which was initially 50 Nm during at the starting of the machine but becomes zero at full speed. Generally, an obvious and cogent observation was the fact that the motor reach it rated speed of 1500 rpm.

4.2 Fault Analysis without Controller

Simulation analysis is conducted in this scenario for single-phase short, two-phase, and three-phase circuits to ground and presented in Fig. 7, 8, and 9, respectively.

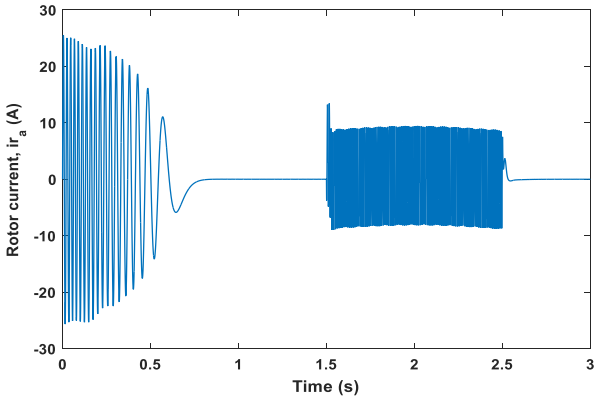

Fig. 7a. *Rotor current for single-phase short circuit fault*

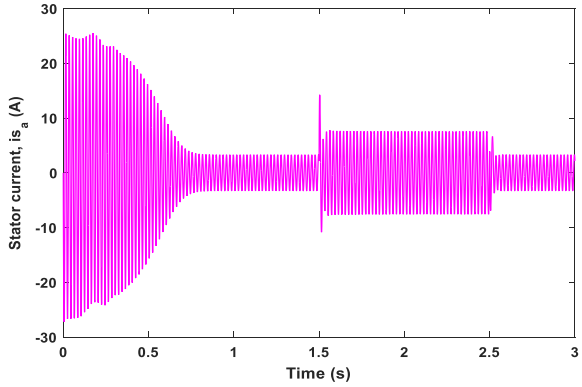

Fig. 7b. *stator current for single-phase short circuit fault*

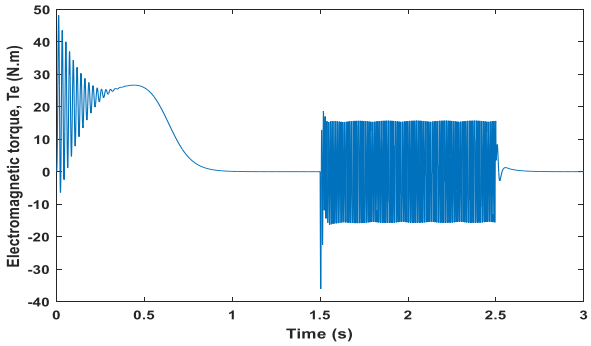

Fig. 7c. *Electromechanical torque for single-phase short circuit fault*

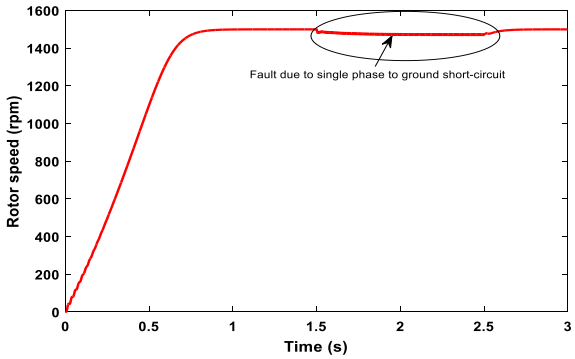

Fig. 7d. *Electromechanical for single-phase short circuit fault*

Fig. 7. *Performance characteristics of the motor due to single-phase short circuit fault*

International Journal of Academic Engineering Research (IJAER)
ISSN: 2643-9085
Vol. 9 Issue 8 August - 2025, Pages: 192-201

With sudden occurrence of single-phase short circuit to ground in the line terminal, resulting effects are shown in Fig. 7. It can be seen that the effect of the single-phase short circuit was increased rotor and stator currents due to heavy current rush associated with short circuit defect and this is obvious within the time the fault occurred at 1.5 second. This consequently resulted in decrease in rotor speed from 1500 rpm to 1470 rpm even though current still flows and the machine keeps running at lower speed.

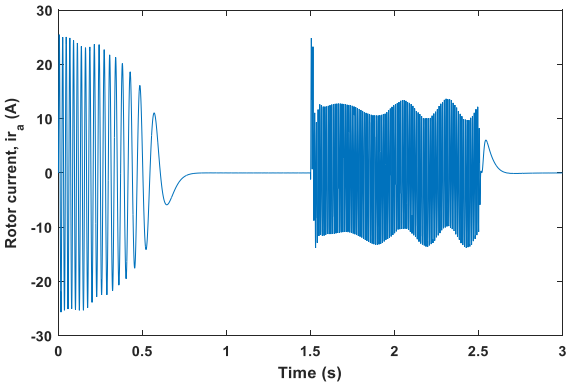

Fig.8a. *Rotor current for two-phase short circuit fault*

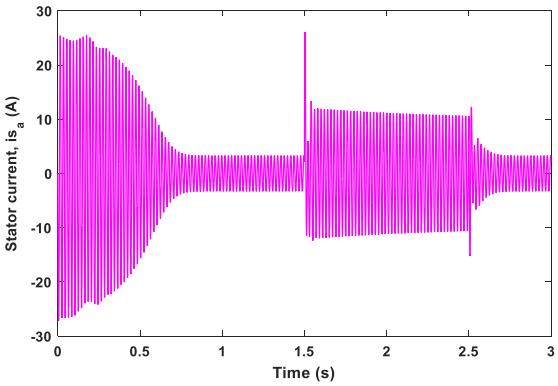

Fig. 8b. *stator current for two-phase short circuit fault*

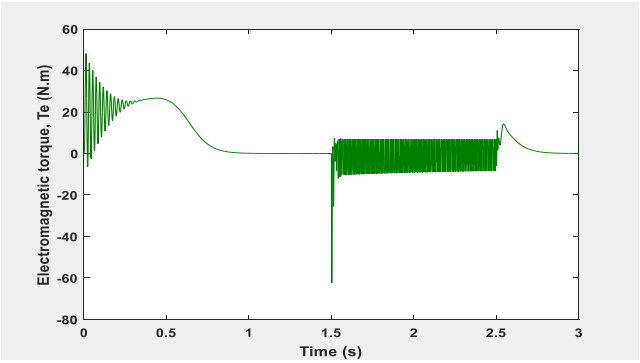

Fig. 8c. *Electromechanical torque for two-phase short circuit fault*

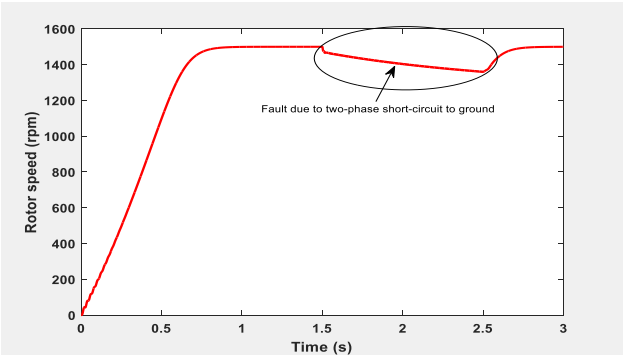

Fig. 8d. *Electromechanical for two-phase short circuit fault*

Fig. 8. *Performance characteristics of the motor due to two-phase short circuit fault*

It can be seen in Figure 8 that the motor behaves almost the same way as with single-phase short circuit scenario. However, since two phases are short circuited to ground, the intensity or magnitude of the short circuit current is further increased at the moment the fault occurred as can be seen with the rotor current and stator current. Thus, with the two-phase to ground short circuit fault, there is more stress or electric pressure entering into the motor at the time of continuity defect. The torque can be seen to have decreased considerably in this fault. The resulting effect is further drop in the motor speed from 1500 rpm to 1365 rpm.

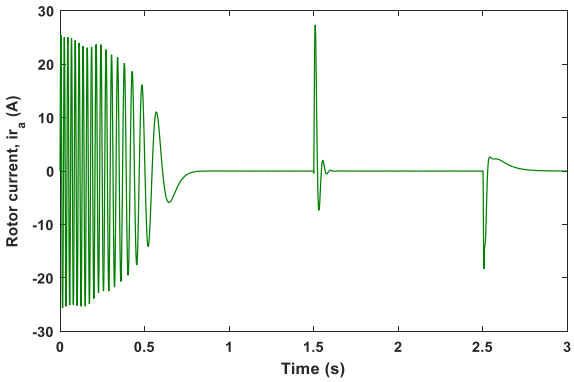

Fig. 9a. Rotor current for three-phase short circuit fault

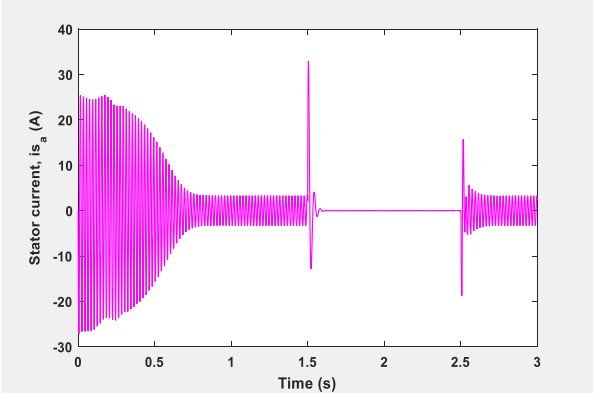

Fig. 9b. stator current for three-phase short circuit fault

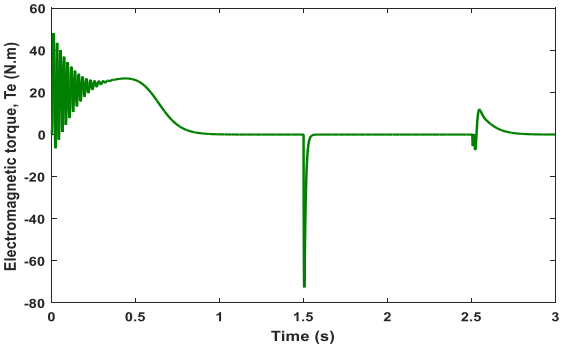

Fig. 9c. Electromechanical torque for three-phase short circuit fault

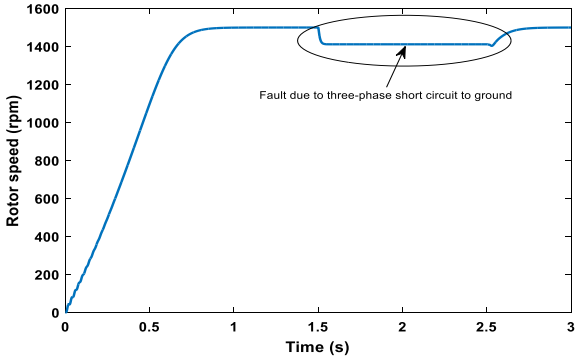

Fig. 9d. Electromechanical for three-phase short circuit fault

Fig. 9. Performance characteristics of the motor due to three-phase short circuit fault

As can be seen in Fig. 9, immediately the three-phase to ground short circuit fault occurred, the rotor current and the stator current increased considerably and reached a very high magnitude at the moment fault occurred compared to the previous mode. However, the current returns to same value as in the case of normal operation after a short while covering the interval of fault. The torque can be seen to have decreased considerably at the time the fault happened but maintained a fixed value just like in the normal operation within the fault interval and then increased considerably after fault period (2.5 seconds) before reducing to zero. The rotor speed decreases from 1500 rpm to 1325 rpm.

4.3 Fault Analysis with the Designed Controller

In this section, the fault detection system for induction motor is implemented with the proposed discrete time PIDf controller. The results of the simulation analysis are shown in Fig. 10. In all cases of short circuit fault, the digital controller triggers the circuit breaker to cut off the supply to the motor which resulted in zero output with respect to the considered performance parameters as illustrated in the various plots.

International Journal of Academic Engineering Research (IJAER)
ISSN: 2643-9085
Vol. 9 Issue 8 August - 2025, Pages: 192-201

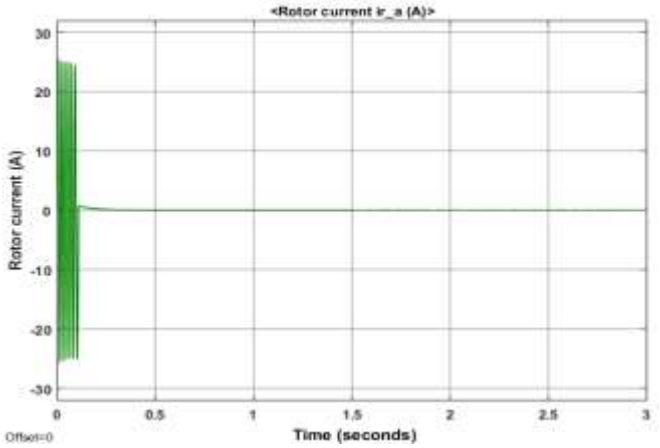

Fig. 10a. *Controller detected rotor current due to short circuit fault*

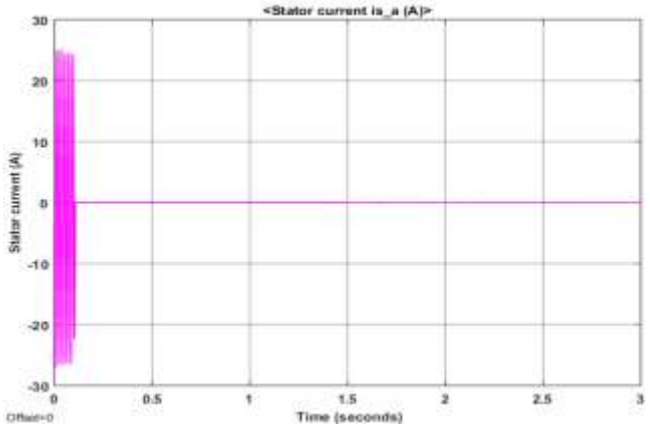

Fig. 10b. *Controller detected stator current due to short circuit fault*

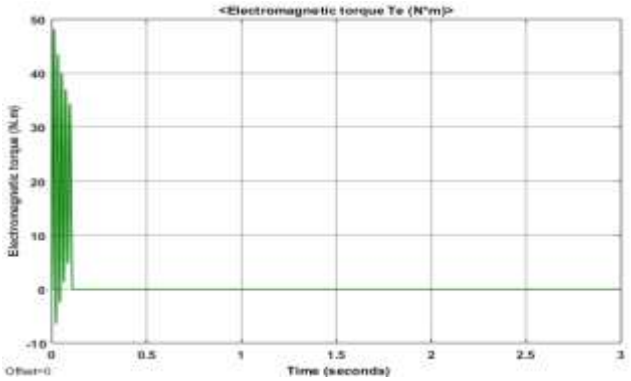

Fig. 10c. *Controller detected electromagnetic torque due to short circuit fault*

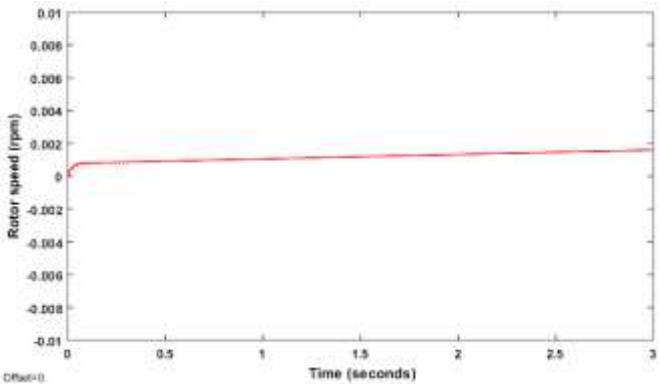

Fig. 10d. *Controller detected rotor speed due to short circuit fault*

Fig. 10. *Performance characteristics of the motor due to short circuit fault with controller*

The simulation results presented in Fig.10 revealed that the rotor current, stator current and electromechanical torque of the motor indicate the effect of start-up current and starting torque (Fig. 10a to 10c) at which point the rotor speed was initially increasing from zero as shown in Fig. 10d, as short circuit fault occurred in the line serving the stator, the measured signal based on RMS technique is fed to the controller, which sensed or detect the error (fault) signal and sent a command signal that ensured the line connection to the motor is tripped off by the circuit breaker. Thus, the resulting output of the motor is zero.

4.4 Signal Analysis

The signal analysis technique used in this work is the RMS method. The graphical analysis showing the nature of the various signals of the motor during normal and faulty operation are shown in Fig. 11 and 12. The RMS expression of the signal during the normal operating condition is shown in Fig. 11, while the signal during faulty condition is shown in Fig. 12 for the three-phase voltages.

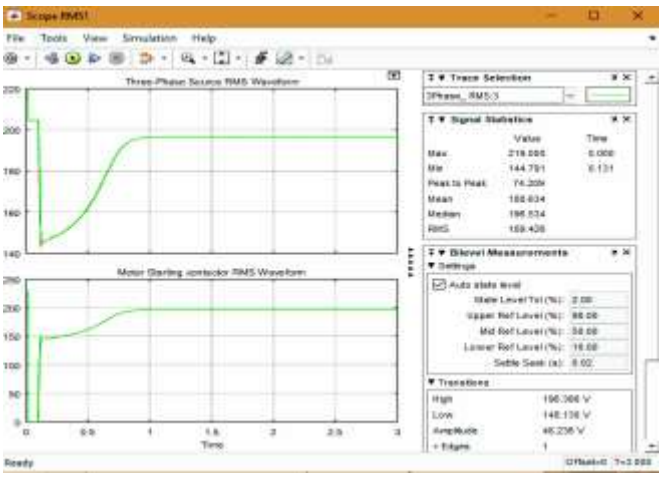

Fig. 11. *RMS waveform of the system during normal operation*

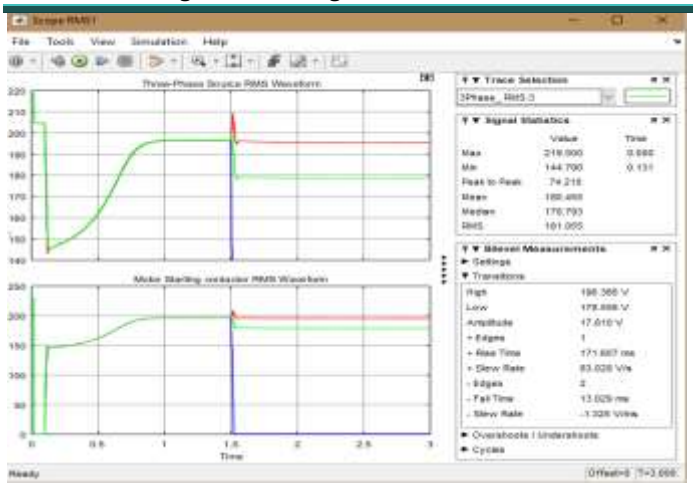

Fig. 12. *RMS waveform of the system during when fault occurred*

In Fig. 11, during the operation of the system when no short circuit has occurred, the signal statistics revealed that the maximum (peak) voltage is 230 V per phase and this was during the starting up while the RMS value was 184.48 V. However, as the motor enters into the transient state the highest voltage measured was 196.650 V and lowest voltage was 1.152 V such that the difference between the two signals gives a signal of amplitude 195.50 V. In Fig. 12, the occurrence of fault initially caused the voltage drop to 219 during the starting state but as the motor entered into its transient mode and kept running, the highest voltage of the signal became 106.366 V and the lowest was 178. 556 V such that measured signal amplitude was 17.810 V. Thus, from the signal analysis it can be seen that the occurrence of fault resulted in dropping of voltage strength or amplitude from 195.50 V to 17.810 V. This drop or sag in voltage amplitude adversely affect the performance of the motor with increased current that can result in overheating.

5. CONCLUSION

As the main components of several industrial and commercial systems, correct and reliable operation and performance of induction is inevitable for efficiency and increased production. Also, having fault detection scheme is of significant and brings valuable advantage by enhancing performance and ensuring that motor is prevented from damage when fault occurs. In this work, a discrete PIDf controller has been design to provide electrical fault detection mechanism for three phase induction motor. The mathematical model of induction motor was determined and Simulink model is used to describe the dynamics of the motor. A PIDf controller was designed with the aid of the MATLAB/Simulink PID tuner. The controller was integrated with the motor network and simulation results revealed that the PIDf ensured that the motor is cut off from the supply line whenever short circuit fault occurs in the network.

REFERENCES

[1] Igbinoba, C. K., & Ofualagba, G. (2020). Design of a three phase induction motor protection system. *Nigerian Research Journal of Engineering and Environmental Sciences, 5*(1), 433-444.

[2] Sudha, M., & Anbalagan, P. (2009). A protection scheme for three-phase induction motor from incipient faults using embedded controller. *Asian Journal of Scientific Research, 2*(1), 28 – 50.

[3] Otor, E., Uju, I. U., Nwosu, A. W., & Imo, F. U. (2024). Enhancing permanent magnet synchronous motor performance characteristics using the combination of vector control and model predictive control. *International Journal of Progressive Research in Engineering, Management and Science, 4*(9),1264-1276.

[4] Asanya, O. N., Uju, I. U., Abonyi, S. E., Ozor, G. O. (2023). Enhancing rotor angle stability of synchronous generators using neuro-fuzzy excitation control model. *International Journal of Latest Technology in Engineering, Management & Applied Science, XII*(IV)

[5] Asiwe, U. M., Uju, I. U., & Iloh, J. P. (2022). Energy consumption minimization of squirrel cage induction motor using classical optimal controller techniques. *Iinternational Journal of Trend in Scientific Research and Development, 6*(4)

[6] Okonkwo, C. G., Uju, I., & Nwajuonye, R. O. (2022). Improvement of three phase induction performance using voltage and frequency speed control techniques. *Journal of Engineering Research and Report, 22*(4), 19-31.

[7] Uneze, I. M., Uju, I. U., & Uneze, C. O. (2023). Dynamic modelling and simulation of single-cage induction machine for transient response performance analysis. *International Journal of Academic multidisciplinary, 7*(11), 251-260.

[8] Uneze, I. M., Uju, I. U., & Uneze, C. O. (2024). Enhancing the transient response of induction motor using double cage rotor model. *International Journal of Academic Engineering Research, 9*(2), 1-10.

[9] Uneze, I. M., Uju, I. U., & Uneze, C. O. (2024).Transient analysis of rotor temperature of single cage and double cage induction motor. *International Research Journal of Advanced Engineering and Science, 8*(5), 100-103.

[10] AL-Bouthigy, R. B., AL-shogairy, A. A., Barkrain, S. Y. M., AL-Qadhi, I. A. M., &Almassabi, M. M. A. (2019). Protection of three phase induction motor using embeddedsystem. *International Journal of Latest Research in Engineering and Technology, 5*(8), 1 – 10.

[11] Boum, A., Maurice, N. Y. J., Nneme, L. N., &Mbumda, L. M. (2018). Fault diagnosis of an induction motor based on fuzzylogic, artificial neural network and hybrid system. *International Journal of Control Science*

and Engineering, 8(2), 42 – 51.https://doi.org/10.5923/j.control.20180802.03

[12] Abubakar, U., Mekhilef, S., Gaeid, K. S., Mokhlis, H., Al Mashhadany, Y. I. (2020). Induction motor fault detection based on multi-sensory control and wavelet analysis. *IET Electric Power Applications, 14*(11), 2051-2061. https://doi.org/10.1049/iet-epa.2020.0030

[13] Kumar, P, Babu, U. N., Kumar, P. V., Raghuram, S., & S. K. Asif, Venkateswarlu, N. (2019). Induction Motor Protection System Using Microcontroller. *International Journal of Research in Engineering, IT and Social Science, 9*(2), 222 – 228.

[14] Mandekar, Y., Bongale, S., Savant, V., Savanti, H., Salunkhe, S., & Pawar, S. (2017). Three phase induction motor protection scheme. *International Research Journal of Engineering and Technology, 4*(3), 747 – 749.

[15] Chouhan, A,,Gangsar, P., Porwal, R., & Mechefske, C. K.(2020).Artificial neural network based fault diagnostics for three phase induction motors under similar operating conditions. *VibroengineeringProcedia, 30*, 55 – 60. https://doi.org/10.21595/vp.2020.21334

[16] Umap, A. A., & Bobade, C. M. (2020). Detection and classification of faults in induction motor using wavelet and fuzzy controller. *International Journal of Advance Research and Innovative Ideas in Education, 6*(4), 674 – 691.

[17] Okoye, U. P., Eze, P. C., & Oyiogu, D. C. (2021). Enhancing the performance of AVR system with prefilter aided PID controller. *Access International Journal of Research & Development, 1*(1), 19-32.

[18] Eze, P. C., Nwadike, S. U., Oyiogu, D. C., & Iroegbu, M. C. (2025). Hybrid PID-LQR controller for dynamic response and stability enhancement of synchronous generator's AVR system. *Asian Journal of Science, Technology, Engineering, Art, 3*(3), 866-879. https://ejournal.yasin-alsys.org/AJSTEA

[19] Ekengwu, B. O., Eze, P. C., Muoghalu, C. N., Asiegbu, C. N., & Achebe, P. N. (2024). Design of robust centralized PID optimized LQR controller for temperature control in single-stage refrigeration system. *Indonesian Journal of Electrical Engineering and Informatics, 12*(3), 726-738. DOI: 10.52549/ijeei.v12i3.5629

[20] Eze, P. C., Njoku, D. O., Nwokonkwo, O. C., Onukwugha, C. G., Odii, J. N., & Jibiri, J. E. (2024). Wheel slip equilibrium point model reference adaptive control based PID controller for antilock braking system: A new approach. *International Journal of Automotive and Mechnical Engineering, 21*(3), 11581-11595.https://doi.org/10.15282/ijame.21.3.2024.10.0893

[21] Eze, P. C., & Ezenugu, I. A. (2024). Microsatellite yaw-axis attitude control system using model reference adaptive control based PID controller. *International Journal of Electrical and Computer Engineering Research, 4*(2), 8–16. https://doi.org/10.53375/ijecer.2024.389

[22] Eze, P. C., Jonathan, A. E., Agwah, B. C. and Okoronkwo, E. A. (2020). Improving the performance response of mobile satellite dish antenna network within Nigeria. *Journal of Electrical, Electronics, Control and Computer Science, 6*(21), 25-30.

[23] Candelo, J. E., & Montaña, J. H. (2016). Voltage sag assessment using an extended fault positions method and Monte Carlo simulation, *DYNA, 83*(195), 180-188.